 doi:10.20944/preprints201811.0052.v1

Article

IgG Charge

Danlin Yang[1], Rachel Kroe-Barrett[1], Sanjaya Singh[2], and Thomas Laue[3,*]

[1] Biotherapeutics Discovery Research, Boehringer Ingelheim Pharmaceuticals, Inc., Ridgefield, Connecticut 06877, USA. Present address: Janssen BioTherapeutics, Janssen Research & Development, LLC, Spring House, Pennsylvania 19477, USA
[2] Janssen BioTherapeutics, Janssen Research & Development, LLC, Spring House, Pennsylvania 19477, USA
[3] Department of Molecular, Cellular and Biomedical Sciences, University of New Hampshire, Durham, New Hampshire, 03861, USA; tom.laue@unh.edu
* Correspondence: tom.laue@unh.edu; Tel.: +01-603-978-5579

Abstract: It has been known since the 1930's that all immunoglobulins carry a weak negative charge in physiological solvents. However, there has been no systematic exploration of this fundamental property. Accurate charge measurements have been made using membrane confined electrophoresis in two solvents (pH 5.0 and pH 7.4) on a panel of twelve mAb IgGs, as well as their F(ab')$_2$ and Fc fragments. The following observations were made at pH 5.0: 1) the measured charge differs from the calculated charge by ~40 for the intact IgGs, and by ~20 for the Fcs; 2) the intact IgG charge depends on both Fv and Fc sequences, but does not equal the sum of the F(ab)'$_2$ and Fc charge; 3) the Fc charge is consistent within a class. In phosphate buffered saline, pH 7.4: 1) the intact IgG charges ranged from 0 to -13; 2) the F(ab')$_2$ fragments are nearly neutral for IgG1s and IgG2s, and about -5 for some of the IgG4s; 3) all Fc fragments are weakly anionic, with IgG1 < IgG2 < IgG4; 4) the charge on the intact IgGs does not equal the sum of the F(ab')$_2$ and Fc charge. In no case is the calculated charge, based on H^+ binding, remotely close to the measured charge. The charge on IgGs in physiological solvent is sufficiently small to minimize its contribution to thermodynamic nonideality. Some of the mAbs carried a charge in physiological salt that was outside the range observed for serum-purified human poly IgG. To best match physiological properties, a therapeutic mAb should have a measured charge that falls within the range observed for serum-derived human IgGs.

Keywords: Analytical electrophoresis; IgG subclasses; monoclonal IgG, Protein charge

1. Introduction

It has been known for over 80 years that all serum proteins, including the immunoglobulins, carry a net negative charge under physiological conditions [1]. More recently, it was shown that freshly prepared human polyclonal IgGs have a Debye-Hückel-Henry charge, Z_{DHH} [2], between -3 and -9 [3]. The narrow range of charge is somewhat surprising since isoelectric focusing analysis of the same sample yielded isoelectric points (pIs) covering the pH range from less than 4 to greater than 10 [3]. Charge is a system property that depends on temperature and solvent composition, and it is believed that the narrow range of Z_{DHH} under physiological conditions is a consequence of anion binding.

It is known that charge and charge distribution are important contributors to protein solubility and solution viscosity [4–7]. The majority of biotherapeutic mAbs exhibit pIs >= 8, and carry a positive charge in the pH 5 – 6 range where they are formulated [5–7]. However, there is no published charge data for these mAbs in physiological solvents, and it is not known whether their charge falls into the range observed for normal human IgGs. It is apparent that a systematic analysis of the charge on mAbs would be useful.

Presented here is an analysis of the charge on twelve anti IL-13 IgGs. Using membrane confined electrophoresis, MCE, charge data have been acquired for three IgGs, mAb1, mAb2 and mAb3, that

 doi:10.20944/preprints201811.0052.v1

bind to different IL-13 epitopes [3]. For each mAb, Z_{DHH} has been measured for four subclasses, IgG1, IgG2, IgG4 and IgG4Pro. Furthermore, the charge on the Fc and F(ab')$_2$ fragments was measured to determine whether the intact IgG charge is the sum of the Fc and F(ab')$_2$ fragment charges, and to assess how the charge is distributed over the IgG structure. Finally, the charge on the IgGs and their fragments were measured at both pH 5.0 and pH 7.4 to determine how the charge varies between formulation and physiological conditions. The results illustrate how little is known about protein charge and demonstrates the power of analytical electrophoresis in assessing this property.

1.1 Background

Protein charge is significant to a variety of biochemical, biophysical and biological phenomena [8]. Thermodynamically, charge is a system property that depends on temperature, pressure, salt concentration, salt type and pH [9]. At present there is no way to calculate protein charge accurately. However, charge may be measured with both precision and accuracy [2,10,11]. Of the measurement methods, membrane confined electrophoresis [12,13] is the most accurate and flexible [2,14].

There are a variety of charge descriptions (e.g. ζ potential, $Z_{effective}$, Z_{DHH}) [2]. While each description is useful, here we will use Z_{DHH}, which is the unitless valence resulting from the ratio of the protein charge (in coulombs) to the proton unit charge (e.g. Ca^{2+} has a valence of +2, Cl^{-1} has a valence of -1). Calculation of Z_{DHH} from the free-boundary electrophoretic mobility removes the effects of electrophoresis and the solvent ion cloud [2,12,15]. Thus, Z_{DHH} reflects any changes in protein charge that accompany changes in solvent pH, salt type or salt concentration [2].

Though pH may contribute to protein charge, Z_{DHH} reflects binding by all solvent ions (e.g. Na^+, PO_4^{2-}, Cl^-) and not just H^+. It has been known for over 60 years that proteins bind anions to a greater extent than cations [16–18]. Two non-exclusive models have emerged for the mechanism of anion binding. One model focuses on the tendency for anions to accumulate preferentially at hydrophobic surfaces [17]. Based on NMR data, the other model suggests that anion binding may involve amide protons [18].

Because ion binding and dissociation occur rapidly, Z_{DHH} values are time averages. The extent of fluctuation about the mean value is proportional to the change in charge with ion chemical potential (i.e. the slope of the curve of Z versus log[X]) [19]. If the titration curve is flat (i.e. dZ/dlog[X] ~0), there will be very little charge variation, and the charge distribution about the average value will be narrow. A steep titration curve, however, indicates large charge variations which, particularly if they swing around neutrality, result in the inter-molecular attractions that reduce solubility and cause higher viscosities. Thus, measurement of Z_{DHH} as a function of solvent ion concentration (including pH) may be helpful in finding solvent conditions that optimize solubility and viscosity.

2. Materials and Methods

2.1. Monoclonal and human serum IgGs

Twelve anti-IL13 IgGs comprising three unique variable regions, each constructed as four human IgG subclasses, IgG1, IgG2, wild-type IgG4(Ser^{222}), and a hinge mutant IgG4(Pro^{222}), were made from stable NS0 cell clone at Boehringer Ingelheim. Human serum derived from male AB plasma was purchased from Sigma (cat# H4522). The IgGs were purified by ÄKTA affinity chromatography system and MabSelect Sure resin (GE Healthcare) following standard methods *[20]*. The quality of the purified mAb IgGs and their fragments generated by subsequent enzymatic digestion was evaluated by analytical size-exclusion ultra-performance liquid chromatography (SE-UPLC) using a BEH200 column on the Waters Acquity UPLC system (Waters Corporation). The mobile phase buffer consisted of 50 mM sodium phosphate (pH 6.8), 200 mM arginine, and 0.05% sodium azide. For each sample run, 10 µg of material was injected onto the column with the running flow rate at 0.5 mL/min for 5 min.

 doi:10.20944/preprints201811.0052.v1

2.2. IgG fragmentation

A FragIT kit with individual spin columns containing the active IdeS, a cycstein protease secreted by *Streptococcus pyogenes* covalently coupled to agarose beads was used (Genovis, cat# A2-FR2-025). After the IgG sample was buffer exchanged into the cleavage buffer (10 mM sodium phosphate, 150 mM NaCl) and the column was equilibrated with the cleavage buffer, the IgG-enzyme mixture was incubated at 37 °C for an hour on an orbital shaker. The digested fragments were separated from the immobilized enzyme, followed by the purification of $F(ab')_2$ using a supplied CaptureSelect column containing Fc affinity matrix (Thermo Fisher). Upon the collection of the $F(ab')_2$ in the flow-through, the Fc was eluted using the 0.1 M glycine (pH 3.0) elution buffer and immediately neutralized by adding 10% v/v of 1 M Tris (pH 8.0).

2.3. Sample preparation

Each sample was dialyzed into desired buffers at 4-10 °C overnight using Zeba desalting columns (Thermo Fischer), after which the concentration was determined using appropriate extinction coefficients in NanoDrop™ 8000 Spectrophotometer (Thermo Fischer). Two solvents were used: 10 mM sodium acetate, 50 mM NaCl, pH 5.0; and Dulbecco's PBS (pH 7.4) containing 8 mM sodium phosphate dibasic, 1.5 mM potassium phosphate monobasic, 2.7 mM KCl, and 138 mM NaCl. The acetate buffer was prepared by diluting chemicals purchased from Sigma into distilled deionized water from a Milli-Q Plus filtration system (Millipore) and titrating to the desired pH 5.0 with 10 N NaOH solution. For all measurements, the sample solutions were used within a week of preparation and stored at 4 °C between measurements.

2.4 Liquid Chromatography Mass Spectrometry (LC-MS)

The sequences of the purified mAbs and respective $F(ab')_2$ and Fc fragments were evaluated by LC-MS using a PoroShell 300SB-C8 column (5 µm, 75 x1.0 mm) on the Agilent HPLC system followed by analysis in the Agilent 6210 time-of-flight mass spectrometer (Agilent Technologies). The composition of the mobile phase A was 99% water, 1% acetonitrile, and 0.1% formic acid, and that of mobile phase B was 95% acetonitrile, 5% water, and 0.1% formic acid. The gradient started with 20% B at 0 min and increased to 85% B at 10 min with the constant flow rate of 50 µl/min. Each sample was subjected to a native run, a reduced run after incubation with TCEP (Sigma), and a deglycosylated run after incubation with TCEP and PNGase F (New England Biolabs). The MassHunter Qualitative Analysis program (version B.06.00) was used to deconvolute the raw data.

2.5 Analytical Ultracentrifugation (AUC)

The solution properties of the purified mAbs and cleaved $F(ab')_2$ and Fc were evaluated by sedimentation velocity experiments in an Optima XL-I AUC equipped with absorbance optics (Beckman Coulter). Each sample was prepared in three concentrations with 1:3 serial dilutions starting from 0.5 mg/mL in the correponding buffer, and 400 µl of the prepared solution was loaded into the sample chamber, whereas buffer was loaded into the reference chamber of an AUC cell assembled with standard double-sector centerpieces and quartz windows. The experiments were conducted at 20 °C using an An60Ti 4-hole rotor spinning at 40,000 rpm. The sedimentation process was monitored by collecting absorbance data at 280 nm wavelength and 30-µm radial increments. The collected data was analyzed using the SEDANAL software by which the apparent sedimentation coefficient distribution g(s*) was derived *[21]*. The resulting analysis was initially plotted as g(s*) vs. s* in which the areas under the peaks provided the concentration for the boundary corresponding to each peak in the distribution. The weight average sedimentation coefficient (s_w) was computed by selecting a range over which to do the average on the plots. The plots were concentration-normalized to enable the inspection for reversible interactions. The Stokes radius, R_s, which is used for Z_{DHH} calculation is derived from the Svedberg equation:

Preprints (www.preprints.org) | NOT PEER-REVIEWED | Posted: 2 November 2018 doi:10.20944/preprints201811.0052.v1

$$R_s = \frac{M(1-\bar{\upsilon}\rho)}{sN_A 6\pi\eta} \quad (1)$$

where M is the molar mass, $\bar{\upsilon}$ is the partial specific volume, ρ is the solvent density, s is the sedimentation coefficient, N_A is the Avogadro's number, and η is the viscosity of the solvent.

2.6. Imaged capillary isoelectric focusing (icIEF)

The pI and charge heterogeneity of the IgG samples were determined on an iCE3 system (Protein Simple) *[22,23]*. Briefly, the pH gradient was created by an ampholyte mixture consisted of 44% (v/v) of 1% methylcellulose, 1.25% (v/v) of pharmalyte 3-10 solution, 3.75% (v/v) µl of pharmalyte 5-8 solution, 1.25% (v/v) of servalyte 9-11 solution, 0.63% (v/v) of pI marker pH 6.14, 0.63% (v/v) of pI marker pH 8.79, 6.3% (v/v) of 200 mM iminodiacetic acid, and 43% (v/v) of water. After sample preparation at 1 mg/mL in DI water, 40 µl of the diluted sample was mixed with 160 µl of ampholyte mixture and centrifuged for 5 min. The operating protocol used an initial potential of 1500 volts for 1 min, followed by a potential of 3000 volts for 20 min. For samples containing highly basic species, pI markers at pH 7.55 and pH 9.77 (0.63% v/v) and a focus period of 10 min at 3000 volts was used. Separation was monitored at 280 nm, and the data analyzed using the iCE CFR software to calibrate the pI values and to select the markers. Subsequetly, the data files were exported to Empower for analysis using the cIEF processing method.

2.7. Membrane-confined electrophoresis (MCE) and Z_{DHH} determinations

Protein valence was measured in the MCE instrument (Spin Analytical), which provides a direct measurement of the electrophoretic mobility (µ) to derive the Z_{eff} and the Z_{DHH} [12,13]. In each experiment, 20 µl of sample at 1 mg/mL was loaded into a 2 x 2 x 4 mm quartz cuvette whose ends were sealed with semipermeable membranes (MWCO 3 kDa, Spectra/Por Biotech grade). An electric field was applied (4.3 V/cm for IgG, 8.5 V/cm for $F(ab')_2$ and Fc, and 19.8 V/cm for serum IgGs) longitudinally across the cell. The applied electric field, *E*, is a function of the applied current, *i*, the buffer conductivity (*κ*, 5.8 mS for 10 mM acetate, 50 mM NaCl [pH 5.0] and 16.8 mS for PBS [pH 7.4]), and the cross-sectional area of the cuvette, *A*, as $E = \frac{i}{\kappa A}$. Image scans of the cuvette were acquired with 25 µm resolution at 280 nm every 10-20 seconds. Time difference analysis provided an apparent electrophoretic mobility distribution, g(µ) versus µ, uncorrected for diffusion. Values of µ were converted to charge using the Spin Analytical software:

$$Z_{eff} = \frac{\mu}{fe} \quad (2)$$

$$Z_{DHH} = Z_{eff}\frac{1+\kappa_D a}{H(\kappa_D a)} \quad (3)$$

where μ is the electrophoretic mobility, *f* is the translational frictional coefficient, *e* is the elementary proton charge , κ_D is the inverse Debye length, *a* is the sum of the Stokes radius of the macromolecule and its counterion (0.18 nm for Cl^{-1} and 0.122 nm for Na^{+}), and $H(\kappa_D a)$ is Henry's function that accounts for electrophoretic effects. For reference, under the experimental conditions used here, $\kappa_D a \sim 2$ and $H(\kappa_D a) \sim 1.1$, though exact values are calculated for each experiment.

2.8 Calculated charge, Z_{Cal}, and calculated isoelectric pH, pI_{Cal}

Sednterp was used to calculate pI values, pI_{Cal}, as well as the H^{+} titration curve from which Z_{Cal} was determined *[24]*. These calculations are based on the amino acid composition and use pKa values from Edsall and Wyman *[25]*. It was assumed that the N-terminal amino groups were not blocked.

 doi:10.20944/preprints201811.0052.v1

2.9 Dynamic light scattering (DLS) and k_D determinations

A DynaPro Plate Reader (Wyatt) running Dynamics (version 7.4.0.72) was used to determine the diffusion interaction parameter, k_D. Each sample was prepared at 5 concentrations ranging from 10 mg/mL to 0.625 mg/mL in 2-fold serial dilutions. 35 µl of each solution was added to a 384-well UV-Star Clear Microplate (Greiner Bio-One), spun in a centrifuge for 2 mins to remove air bubbles and then placed into the plate reader. The experiment was started after the temperature inside the reader reached 20 °C. A total of 10 acquisitions at 20 s per acquisition were obtained for each sample. A well image was acquired after the last acquisition measurement to look for bubbles or deposited aggregates. The mutual diffusion coefficient (D_m) was plotted against the sample concentration $D_m=D_0(1+k_Dc)$, with D_0 and k_D determined by linear regression analysis using GraphPad Prism (version 7.03). The error for k_D was determined by calculating the propagation of the standard error of the coefficients from the linear regression.

3. Results

All purified IgGs contain > 99% monomer content as assessed by analytical SE-UPLC and are sequence confirmed by LC-MS. These twelve mAbs also displayed homogeneous solution properties within each mAb group in both pH 5.0 acetate and pH 7.4 PBS buffer conditions as illustrated in Figure 1. Overlaps between the IgG subclasses within each mAb group are observed, in which the weight-average sedimentation coefficients (s_w) are 6.37 ± 0.06, 6.37 ± 0.05, and 6.43 ± 0.09 in pH 5.0 acetate, and 6.28 ± 0.04, 6.27 ± 0.07, and 6.31 ± 0.06 in pH 7.4 PBS for mAb 1, mAb 2, and mAb 3, respectively. These s_w values are consistent with the molecular weight of ~150 kDa IgG antibodies.

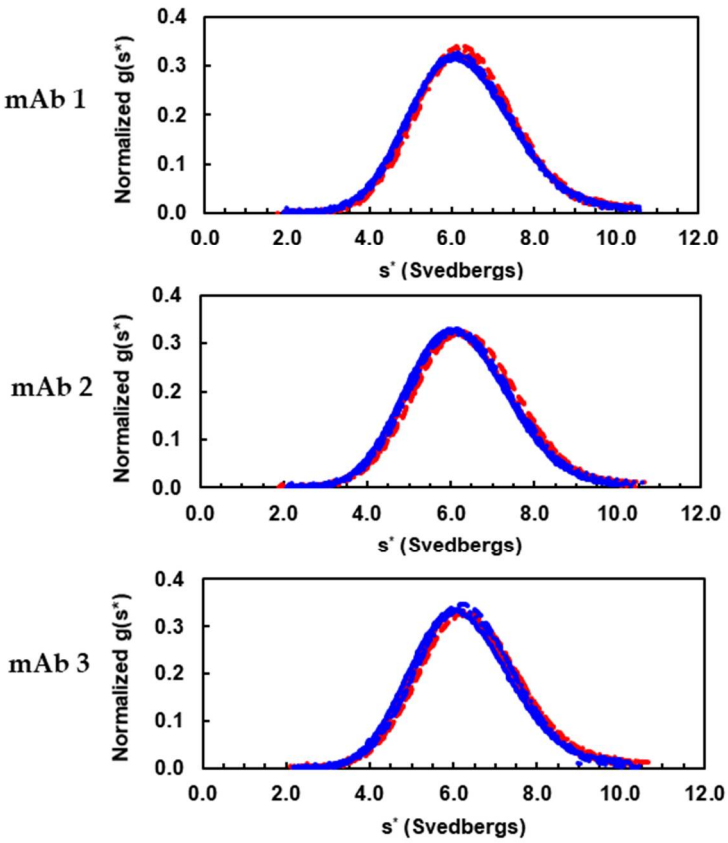

Figure 1. Sedimentation velocity analysis of IgG subclasses from mAb1, mAb2, and mAb3 in pH 5.0 acetate (red) and pH 7.4 PBS (blue) solutions. Normalized g(s*) sedimentation distributions are obtained from IgG1 (solid line), IgG2 (dotted line), IgG4 (dashed line), and IgG4Pro (dot-dashed line) in both buffers. The

Preprints (www.preprints.org) | NOT PEER-REVIEWED | Posted: 2 November 2018 doi:10.20944/preprints201811.0052.v1

purity assessed by SE-UPLC and cleavage sites between F(ab')$_2$ and Fc identified by LC-MS are summarized in Table 1.

Table 1. Quality of IgG fragments from IdeS digestion.

Subclass	V region	Cleaved Site	F(ab')$_2$ purity (%)	Fc purity (%)
IgG1	mAb 1	…CPPCPAPELLG / GPSVF…	95	100
	mAb 2		100	
	mAb 3		100	
IgG2	mAb 1	…CPPCPAPPVA / GPSVF…	100	98
	mAb 2		100	
	mAb 3		100	
IgG4	mAb 1	…CPSCPAPELLG / GPSVF…	95	97
	mAb 2		95	
	mAb 3		97	
IgG4Pro	mAb 1	…CPPCPAPELLG / GPSVF…	97	
	mAb 2		100	
	mAb 3		100	

The solution homogeneity of each cleaved fragment was assessed by SV-AUC. All IgG fragments showed sedimentation distribution profiles like that in Figure 2 for mAb 1, where the superposition of the three concentrations of F(ab')$_2$ and Fc samples indicate homogeneity and the absence of self-association. The weight-average sedimentation coefficients (s_w) from the Fc evaluations are 3.45 ± 0.02, 3.46 ± 0.02, and 3.38 ± 0.18 for IgG1, IgG2, and IgG4, respectively. These values are consistent with the molecular weight of ~50 kDa, which indicates Fc homodimer in solution despite cleavage below the hinge region. The s_w from the F(ab')$_2$ evaluations are 4.86 ± 0.01, 5.14 ± 0.06, 4.90 ± 0.02, and 4.95 ± 0.01 for IgG1, IgG2, IgG4, and IgG4Pro, respectively. These values are consistent with the molecular weight of ~100 kDa, which is expected for a bivalent Fab linked by hinge.

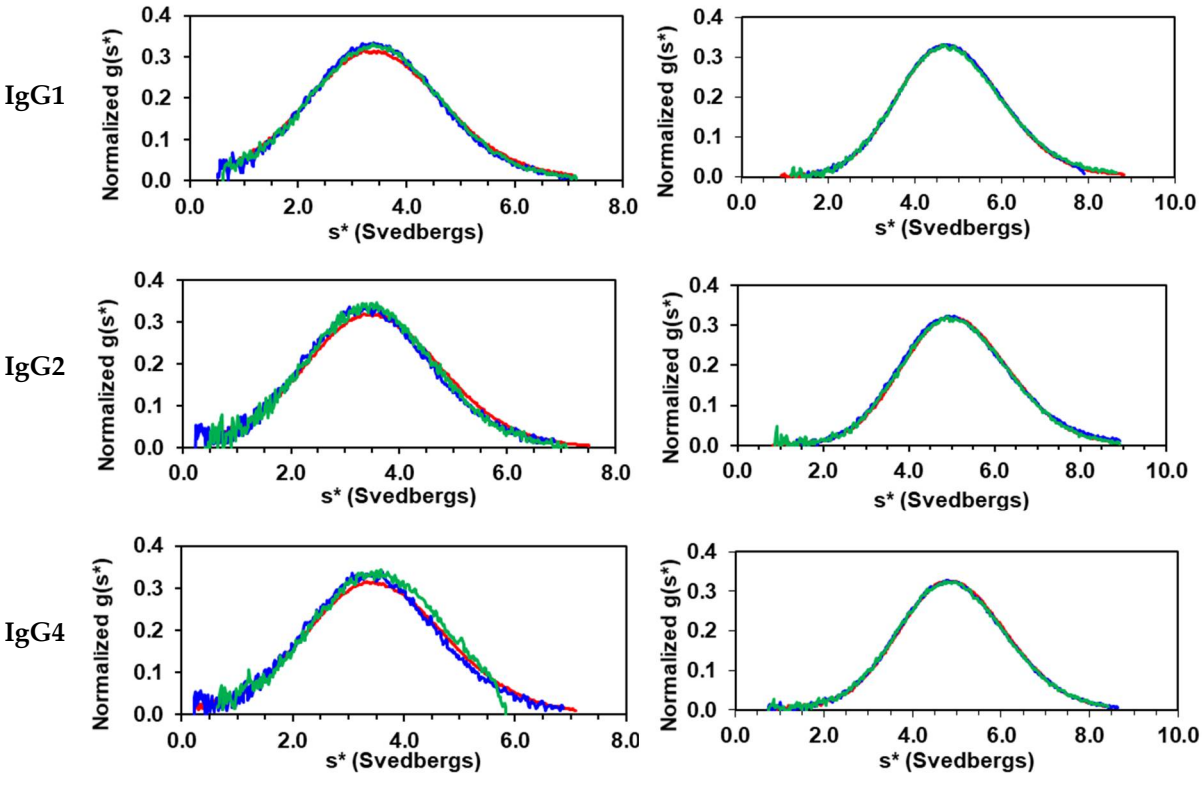

Preprints (www.preprints.org) | NOT PEER-REVIEWED | Posted: 2 November 2018 doi:10.20944/preprints201811.0052.v1

Figure 2. Sedimentation velocity analysis of IgG1, IgG2, and IgG4 cleaved (a) Fc and (b) F(ab')$_2$ from mAb1 in pH 5.0 acetate. Normalized g(s*) sedimentation distributions obtained with the concentration of 0.5 mg/mL (red), 0.167 mg/mL (blue), and 0.056 mg/mL (green).

All IgGs exhibited pI profiles like that in Figure 3 for mAb1 IgG1. Three-peaks are observed, acidic, main and basic. The pI values for each IgG are presented in Table 2, along with the calculated pI. For each mAb, the subclass pIs followed the trend: IgG1 > IgG2 > IgG4, with those of IgG4 and IgG4Pro being identical. The measured main species pI and the calculated pI are correlated (Figure 4), though the intercept (-1) suggests that pI$_{Cal}$ corresponds to the more acidic species.

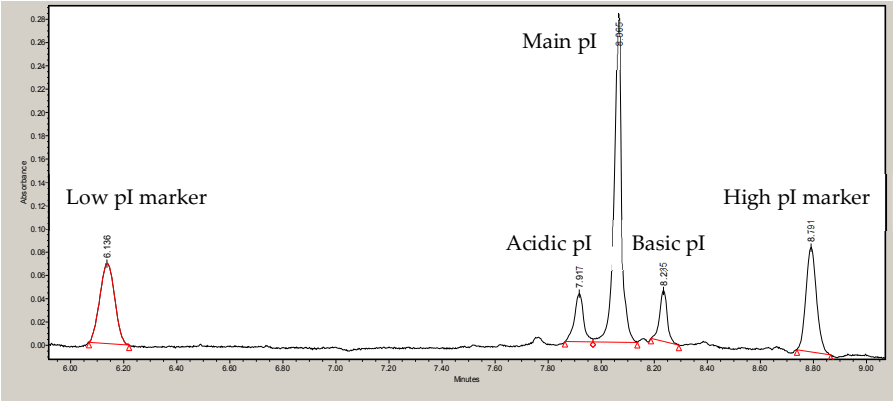

Figure 3. Electrophoretogram image of mAb1 IgG1. The peaks to the left and to the right of the main peak indicates acidic and basic charge variant, respectively.

Table 2. Measured and calculated pI values of IgG.

ID	Subclass	pI$_{cal}$*	pI$_{icIEF}$		
			Acidic peak	Main peak	Basic peak
mAb1	IgG1	7.7	7.9	8.1	8.2
	IgG2	6.9	6.9	7.0	7.3
	IgG4	6.6	6.2	6.3	6.5
	IgG4Pro	6.6	6.2	6.3	6.5
mAb2	IgG1	8.2	8.2	8.4	8.6
	IgG2	7.3	7.9	8.0	8.2
	IgG4	7.0	7.4	7.6	7.7
	IgG4Pro	7.0	7.4	7.6	7.7
mAb3	IgG1	8.2	8.2	8.4	8.6
	IgG2	7.4	7.2	8.0	8.1
	IgG4	7.1	7.5	7.7	7.8
	IgG4Pro	7.1	7.5	7.7	7.8

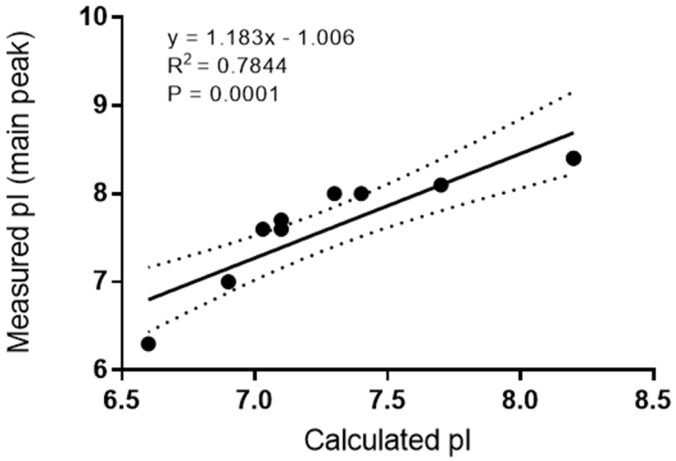

Preprints (www.preprints.org) | NOT PEER-REVIEWED | Posted: 2 November 2018 doi:10.20944/preprints201811.0052.v1

Figure 4. Linear regression analysis and correlation between experimental pI as measured by icIEF and theoretical pI calculated from the IgG sequence. Dotted lines indicate the 95% confidence interval.

Using MCE, the electrophoretic mobility was determined for each IgG and its cleaved F(ab')$_2$ and Fc in pH 5.0 acetate and pH 7.4 PBS as illustrated in Figure 5. By applying the Debye-Hückel approximation to correct for the solvent shielding effects, Henry's function to correct for electrophoretic effects, and using the sum of the measured protein Stokes radius and its counterion, the Z_{DHH} distribution may be calculated from the electrophoretic mobility (Figure 5, right-hand panels).

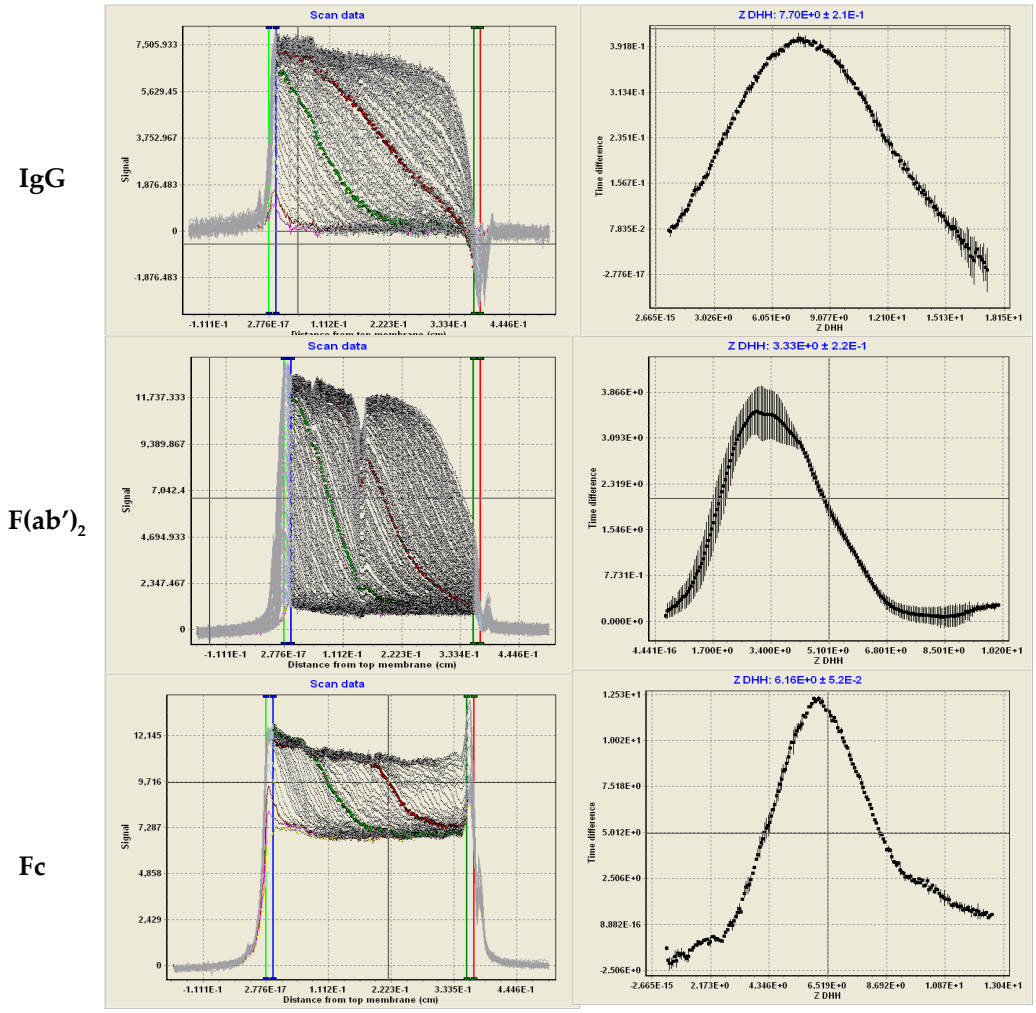

Figure 5. Z_{DHH} determination of IgG, F(ab')$_2$, and Fc by MCE in pH 5.0 acetate. (**a**) Raw MCE scans over time during electrophoresis. The data (left panel) shows the light intensity (I, vertical axis) as a function of the distance moved from the membrane (cm, horizontal). Time difference curves ($\Delta I/\Delta t$) are calculated from data between the green and red highlighted scans. The electrophoretic mobility distribution is calculated from distance moved from the membrane, x, divided by the product of the electric field, E, and average elapsed time for the middle scan $\bar{t}$, $\mu = \frac{x}{E \cdot \bar{t}}$. (**b**) The vertical axis shows the time derivative ($\Delta I/\Delta t$) of the intensity data in panel (a) as a function of Z_{DHH} (horizontal axis). Z_{DHH} was calculated from the mobility using T = 20 °C; viscosity = 0.98 cp; conductance = 16.8 mS; E = -19.8 V/cm, D = 78; counterion radius, 0.18 nm; Stokes radius, 5.5 nm. The peak Z_{DHH} position is displayed above the curve.

Table 3 and Table 4 summarize the Z_{DHH} measurements, as well as the calculated charge, Z_{Cal}, in pH 5.0 acetate and pH 7.4 PBS, respectively. A 0 charge was assigned if no boundary formed

Preprints (www.preprints.org) | NOT PEER-REVIEWED | Posted: 2 November 2018 doi:10.20944/preprints201811.0052.v1

during electrophoresis regardless of the E field direction or magnitude. In acetate pH 5.0 all IgGs and their fragments are cationic (Table 3). However, in all cases the measured Z_{DHH} is substantially lower than Z_{cal}. In PBS pH 7.4 (Table 4), all intact IgGs are neutral (Mab2/IgG1) or anionic, despite the fact the Z_{cal} is cationic in some cases. For all mAbs, Z_{DHH} decreases with subclass in the rank order of IgG1 > IgG2 > IgG4.

Table 3. Measured and calculated Z values of IgG, F(ab')$_2$, and Fc in pH 5.0 acetate.

ID	Subclass	IgG		F(ab')$_2$		Fc	
		Z_{DHH}	Z_{cal}	Z_{DHH}	Z_{cal}	Z_{DHH}	Z_{cal}
mAb 1	IgG1	7.7 ± 0.2	57.3	3.3 ± 0.2	31.2	6.2 ± 0.1[a]	26.30
	IgG2	3.9 ± 0.1	50.0	0	25.9	4.9 ± 0.1[b]	24.30
	IgG4	1.4 ± 0.2	46.7	1.3 ± 0.1	27.9	0.45 ± 0.1[c]	18.98
	IgG4Pro	1.4 ± 0.8	46.7	1.5 ± 0.2	27.9	[c]	
mAb 2	IgG1	10.6 ± 0.1	61.0	8.6 ± 0.2	34.9	[a]	
	IgG2	10.1 ± 0.2	53.7	4.7 ± 0.1	29.6	[b]	
	IgG4	5.6 ± 0.2	50.4	6.2 ± 0.1	31.6	[c]	
	IgG4Pro	5.6 ± 0.2	50.4	6.2 ± 0.1	31.6	[c]	
mAb 3	IgG1	12.5 ± 0.1	65.8	9.4 ± 0.1	39.6	[a]	
	IgG2	10.3 ± 0.2	58.5	5.3 ± 0.2	34.3	[b]	
	IgG4	7.7 ± 0.2	55.1	7.1 ± 0.1	36.3	[c]	
	IgG4Pro	7.8 ± 0.2	55.1	7.3 ± 0.1	36.3	[c]	

[a]pooled IgG1-Fc dialyzed into acetate from mAb1, mAb2, and mAb3 digestions

[b]pooled IgG2-Fc dialyzed into acetate from mAb1, mAb2, and mAb3 digestions

[c]pooled IgG4-Fc dialyzed into acetate from mAb1, mAb2, and mAb3 digestions

Table 4. Measured and calculated Z values of IgG, F(ab')$_2$, and Fc in pH 7.4 PBS.

ID	Subclass	IgG		F(ab')$_2$		Fc	
		Z_{DHH}	Z_{cal}	Z_{DHH}	Z_{cal}	Z_{DHH}	Z_{cal}
mAb 1	IgG1	-5.6 ± 0.1	1.8	0	-0.48	-2.8 ± 0.1[d]	1.50
	IgG2	-7.7 ± 0.6	-4.4	0	-4.59	-6.0 ± 0.6[e]	-0.48
	IgG4	-10.6 ± 0.5	-6.5	-4.3 ± 0.8	-2.61	-10.4 ± 0.3[f]	-4.60
	IgG4Pro	-13 ± 0.3	-6.5	-5.05 ± 0.5	-2.61	[f]	
mAb 2	IgG1	0	5.8	0	3.5	[d]	
	IgG2	-3.2 ± 0.2	-0.4	0	-0.61	[e]	
	IgG4	-7.4 ± 0.2	-2.5	0	1.38	[f]	
	IgG4Pro	-9.6 ± 0.4	-2.5	0	1.38	[f]	
mAb 3	IgG1	-5.3 ± 0.5	6.0	0	3.45	[d]	
	IgG2	-6.1 ± 0.3	-0.1	0	-0.36	[e]	
	IgG4	-6.1 ± 0.2	-2.2	0	1.63	[f]	
	IgG4Pro	-10.7 ± 0.4	-2.2	0	1.63	[f]	

[d]pooled IgG1-Fc dialyzed into PBS from mAb1, mAb2, and mAb3 digestions

[e]pooled IgG2-Fc dialyzed into PBS from mAb1, mAb2, and mAb3 digestions

[f]pooled IgG4-Fc dialyzed into PBS from mAb1, mAb2, and mAb3 digestions

While Z_{DHH} and Z_{cal} are correlated in either solvent (Figure 6), the slope is about ½ - ¾ of what would be expected if there were a 1:1 correspondence between the expected H^+ uptake/release and Z_{DHH}. These data are consistent with a model in which an anion is bound for every 1.3 – 2 H^+ bound. Similarly, Z_{DHH} for the intact IgGs correlates with the sum of Z_{DHH} from fragments (Figure 7), albeit with a slope that is about ½ of that expected if the charge on the fragments simply summed. We

Preprints (www.preprints.org) | NOT PEER-REVIEWED | Posted: 2 November 2018 doi:10.20944/preprints201811.0052.v1

have no mechanism or explanation for the data in Figure 7 and present them here in the hope that they will encourage future work.

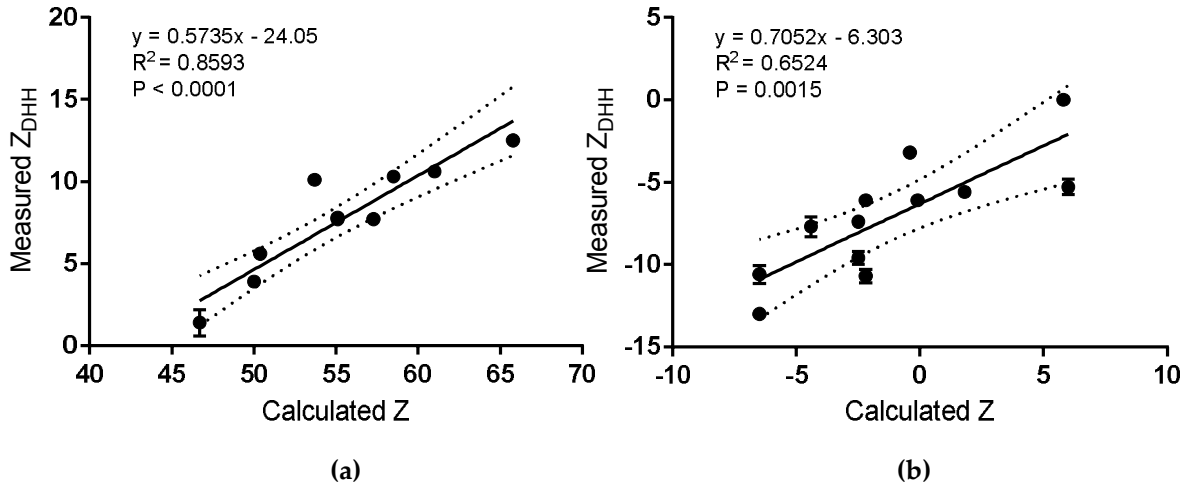

(a) (b)

Figure 6. Linear regression analysis and correlation between experimental Z_{DHH} measured by MCE and theoretical Z calculated from the IgG sequence. (a) pH 5.0 acetate. (b) pH 7.4 PBS. Dotted lines indicate the 95% confidence interval.

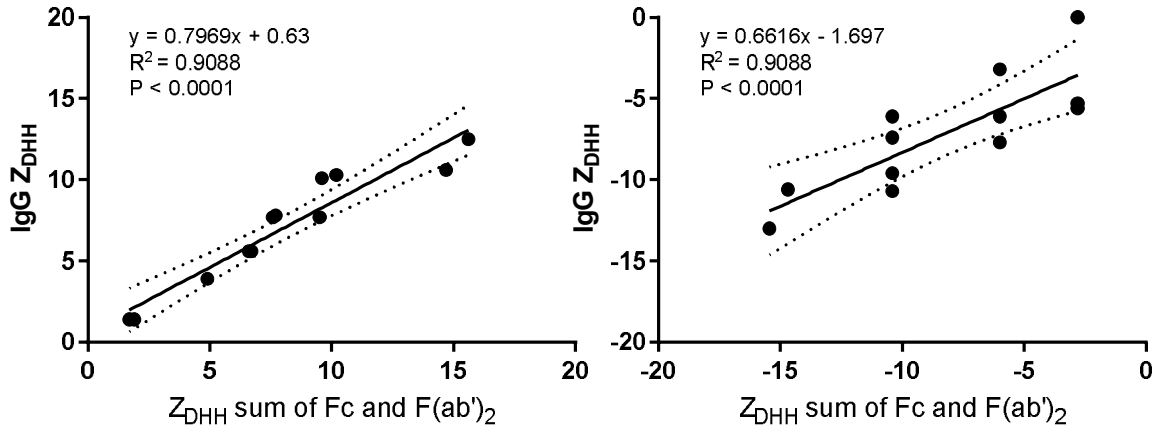

(a) (b)

Figure 7. Linear regression analysis and correlation between Z_{DHH} measured from intact IgG and the sum of Z_{DHH} from the fragments. (a) pH 5.0 acetate. (b) pH 7.4 PBS. Dotted lines indicate the 95% confidence interval.

4. Discussion

Protein charge directly influences the structure, stability, solubility, and ability to interact with other macromolecules [26]. Charge-charge repulsion is important for overcoming the attractive forces that lead to high viscosities in high-concentration protein solutions [27]. Because protein charge can vary with solvent conditions, it is a *system* property rather than a property of the protein. The systematic analysis of twelve mAbs and their F(ab')$_2$ and Fc fragments provides several insights into IgG charge and raises several important questions about our understanding of protein charge.

Charge-charge repulsion contributes to thermodynamic nonideality and, consequently, the colloidal stability of protein solutions [9]. It is clear from the data in Tables 3 and 4 that charge

Preprints (www.preprints.org) | NOT PEER-REVIEWED | Posted: 2 November 2018 doi:10.20944/preprints201811.0052.v1

calculations based solely on H^+ binding lead to highly inaccurate estimates of IgG charge. Thus, even though there is a correlation between the measured and calculated charge (Figure 6), charge calculations should not be considered reliable. Given its potential importance to colloidal stability, it is important to determine the impact of charge on nonideality.

At low to moderate protein concentrations (< ~15 mg/mL), the net sum of all repulsive and attractive interactions is described by the second virial coefficient, B_{22} or A_2. The diffusion interaction parameter, k_D, is related to and often used as a stand-in for these quantities [28], with more positive values of k_D correlating with more positive values of B_{22}, i.e. greater repulsive interactions. If charge-charge repulsion contributes significantly to nonideality, there should be a positive correlation of charge with k_D. Figure 8 shows the correlation of Z_{DHH} with the diffusion interaction parameter, k_D. Under formulation conditions (Figure 6, panel a) increasing Z_{DHH} correlates with increased repulsive interaction (i.e. k_D becomes more positive). This suggests that charge measurements may be a useful parameter for selecting candidate mAbs for development. It should be noted that it is the effective charge, Z_{eff}, rather than Z_{DHH}, that impacts thermodynamic nonideality [2]. This distinction is important because Z_{eff} includes the contribution of the solvent ions, with Z_{eff} decreasing (i.e. repulsive interactions decreasing) as salt concentration is increased [9]. Because salt diminishes charge-charge interactions, thus reducing colloidal stability, it should be no surprise that most mAbs are manufactured and formulated in low-salt solvents.

While charge does contribute to nonideality under formulation conditions, there is no correlation between Z_{DHH} and k_D under physiological conditions (Figure 8, panel b). This result means that it is unfavorable solvent displacement energies that keep mAbs in solution, for all other protein-protein interactions are attractive [29]. Similarly, it is likely that it is the protein solvation shell that dominates the solubility of serum IgG.

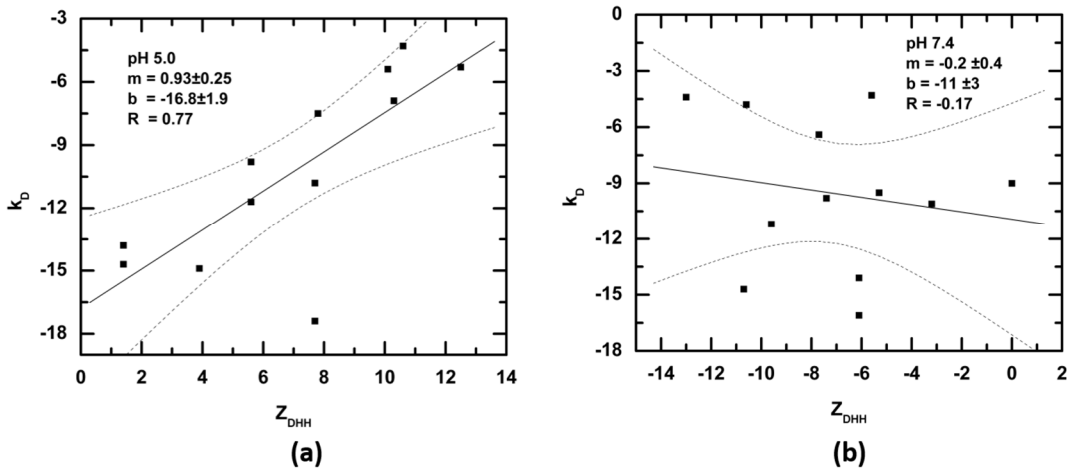

Figure 8. Linear regression analysis and correlation between Z_{DHH} measured for intact IgG and the concentration-dependence of the diffusion coefficient, k_D. (b) pH 7.4 PBS. Dotted lines indicate the 95% confidence interval.

One surprising result of our work is that freshly prepared human IgG exhibits a rather narrow Z_{DHH} distribution in physiological solvent (from approximately -10 to -2, Figure 9), even though isoelectric focusing shows that the same sample has species ranging from pI < 4 to pI > 10. **[30]** This exact same Z_{DHH} range may be calculated from electrophoretic mobility measurements published 80 years ago [1]. Figure 9 shows that most, but not all, of the mAbs in this study exhibit Z_{DHH} that fall

Preprints (www.preprints.org) | NOT PEER-REVIEWED | Posted: 2 November 2018 doi:10.20944/preprints201811.0052.v1

in the range for human serum poly IgG. It is not clear whether there are any physiological or medical consequences associated with a mAb Z_{DHH} that falls outside the normal physiological range. Thus, these results are presented in the hopes of stimulating further research.

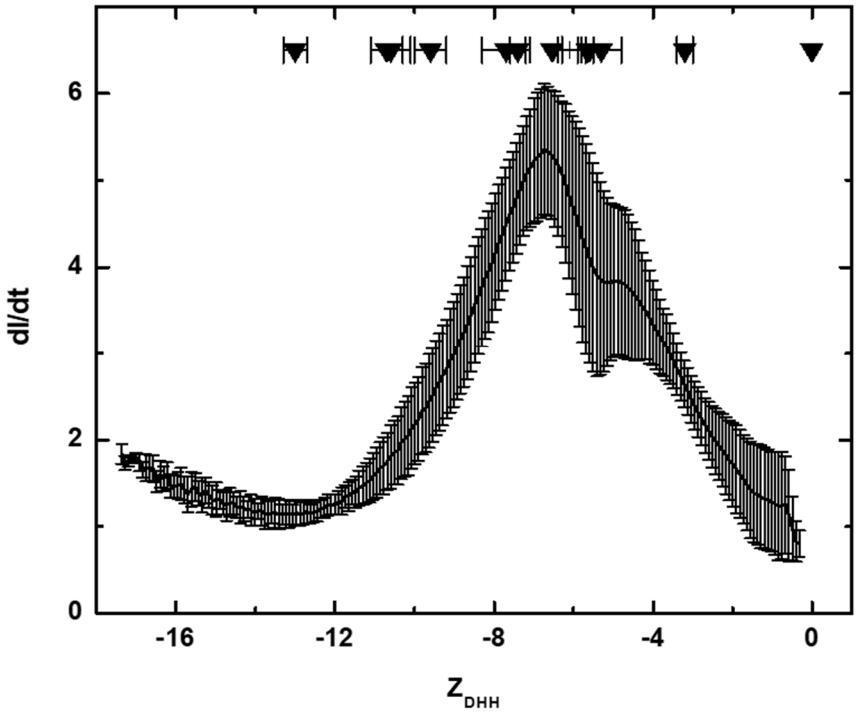

Figure 9. Z_{DHH} distribution for freshly prepared human IgG in DPBS. Z_{DHH} was calculated for T = 20 °C, viscosity = 0.98 cp, electric field = -14.88 V/cm, ionic strength = 0.167 M, conductivity = 16.6 ms, protein radius = 5.5 nm, counterion radius = 0.18 nm, D = 78. The Z_{DHH} for the twelve intact IgGs in this study are noted (inverted triangles) along with bars indicating the measurement uncertainty.

5. Conclusions

Protein charge contributes to producing the colloidally stable mAb solutions needed during development, manufacture and formulation. At this time, protein charge cannot be calculated with any accuracy by even the most detailed structural information using the most sophisticated algorithms. Protein charge, however, is readily measured with accuracy and precision. In this first systematic and comprehensive examination of the charge on IgGs it is clear that: 1) IgGs bind significant quantities of anions, 2) anion binding will contribute to the desolvation energy, thus preventing IgG aggregation, 3) mAb charge measurements may be useful in selecting candidate molecules for development and 4) mAb charge measurements under physiological conditions may be useful in determining whether a candidate molecule falls within the normal range for human IgGs.

Author Contributions: Conceptualization, D.Y., T.L., S.S., and R.K-B.; Methodology, T.L and D.Y.; Analysis, D.Y. T.L.; Investigation, D.Y.; Resources, R.K-B.; Writing-Original Draft Preparation, D.Y and T.L.; Writing-Review & Editing, R.K-B. and S.S.; Supervision, R.K-B. and T.L.; Project Administration, R.K-B. and T.L.; Funding Acquisition, R.K-B and S.S..

Funding: Boehringer-Ingelheim

Acknowledgments: The authors wish to thank Boehringer-Ingelheim for supporting the doctorate research of Danlin Yang, a portion of which is published here. Special thanks to her Ph.D. committee members, David Hayes and Christopher Roberts, who encouraged this work and offered helpful advice. We also are thankful for the encouragement and interest expressed by the members of the Biomolecular Interactions Technology Center (BITC). This paper is dedicated to the memory of Eric and Betty Laue.

Conflicts of Interest: The authors declare no conflict of interest.

References

1. Tiselius, A.; Kabat, E. A. An electrophoretic study of immune sera and purified antibody preparations. *J. Exp. Med.* **1939**, *69*, 119–131.
2. Filoti, D. I.; Shire, S. J.; Yadav, S.; Laue, T. M. Comparative study of analytical techniques for determining protein charge. *J. Pharm. Sci.* **2015**, *104*, 2123–2131, doi:10.1002/jps.24454.
3. Yang, D.; Correia, J. J.; Iii, W. F. S.; Roberts, C. J.; Singh, S.; Hayes, D.; Kroe-Barrett, R.; Nixon, A.; Laue, T. M. Weak IgG self- and hetero-association characterized by fluorescence analytical ultracentrifugation. *Protein Sci.* **2018**, *27*, 1334–1348, doi:10.1002/pro.3422.
4. Cohn, E. J. Studies in the physical chemistry of the proteins: I. the solubility of certain proteins at their isoelectric points. *J. Gen. Physiol.* **1922**, *4*, 697–722, doi:10.1085/jgp.4.6.697.
5. Raut, A. S.; Kalonia, D. S. Opalescence in Monoclonal Antibody Solutions and Its Correlation with Intermolecular Interactions in Dilute and Concentrated Solutions. *J. Pharm. Sci.* **2015**, *104*, 1263–1274, doi:10.1002/jps.24326.
6. Shire, S. J.; Shahrokh, Z.; Liu, J. Challenges in the development of high protein concentration formulations. *J. Pharm. Sci.* **2004**, *93*, 1390–1402, doi:10.1002/jps.20079.
7. Li, L.; Kumar, S.; Buck, P. M.; Burns, C.; Lavoie, J.; Singh, S. K.; Warne, N. W.; Nichols, P.; Luksha, N.; Boardman, D. Concentration dependent viscosity of monoclonal antibody solutions: explaining experimental behavior in terms of molecular properties. *Pharm. Res.* **2014**, *31*, 3161–3178, doi:10.1007/s11095-014-1409-0.
8. Mathews, C. K.; Holde, K. E. van; Appling, D. R.; Anthony-Cahill, S. J. *Biochemistry*; 4 edition.; Pearson: Toronto, 2012; ISBN 978-0-13-800464-4.
9. Tanford, C. *Physical Chemistry of Macromolecules*; First Edition edition.; John Wiley & Sons Inc: New York, 1961; ISBN 978-0-471-84447-1.
10. Moody, T. P.; Kingsbury, J. S.; Durant, J. A.; Wilson, T. J.; Chase, S. F.; Laue, T. M. Valence and anion binding of bovine ribonuclease A between pH 6 and 8. *Anal. Biochem.* **2005**, *336*, 243–252, doi:10.1016/j.ab.2004.09.009.
11. Her, C.; Filoti, D. I.; McLean, M. A.; Sligar, S. G.; Alexander Ross, J. B.; Steele, H.; Laue, T. M. The Charge Properties of Phospholipid Nanodiscs. *Biophys. J.* **2016**, *111*, 989–998, doi:10.1016/j.bpj.2016.06.041.
12. Ridgeway, T. M.; Hayes, D. B.; Moody, T. P.; Wilson, T. J.; Anderson, A. L.; Levasseur, J. H.; Demaine, P. D.; Kenty, B. E.; Laue, T. M. An apparatus for membrane-confined analytical electrophoresis. *Electrophoresis* **1998**, *19*, 1611–1619, doi:10.1002/elps.1150191016.
13. Laue, T. M.; Shepard, H. K.; Ridgeway, T. M.; Moody, T. P.; Wilson, T. J. Membrane-confined analytical electrophoresis. *Methods Enzymol.* **1998**, *295*, 494–518.
14. Kyne, C.; Jordon, K.; Filoti, D. I.; Laue, T. M.; Crowley, P. B. Protein charge determination and implications for interactions in cell extracts. *Protein Sci. Publ. Protein Soc.* **2017**, *26*, 258–267, doi:10.1002/pro.3077.
15. Moody, T. P.; Shepard, H. K. Nonequilibrium thermodynamics of membrane-confined electrophoresis. *Biophys. Chem.* **2004**, *108*, 51–76, doi:10.1016/j.bpc.2003.10.009.
16. Scatchard George The attractions of proteins for small molecules and ions. *Ann. N. Y. Acad. Sci.* **1949**, *51*, 660–672, doi:10.1111/j.1749-6632.1949.tb27297.x.

17. Gokarn, Y. R.; Fesinmeyer, R. M.; Saluja, A.; Razinkov, V.; Chase, S. F.; Laue, T. M.; Brems, D. N. Effective charge measurements reveal selective and preferential accumulation of anions, but not cations, at the protein surface in dilute salt solutions. *Protein Sci. Publ. Protein Soc.* **2011**, *20*, 580–587, doi:10.1002/pro.591.
18. Miao, L.; Qin, H.; Koehl, P.; Song, J. Selective and specific ion binding on proteins at physiologically-relevant concentrations. *FEBS Lett.* **2011**, *585*, 3126–3132, doi:10.1016/j.febslet.2011.08.048.
19. Edsall, J. T.; Wyman, J. Chapter 9 - Polybasic Acids, Bases, and Ampholytes, Including Proteins. In *Biophysical Chemistry*; Edsall, J. T., Wyman, J., Eds.; Academic Press, 1958; pp. 477–549 ISBN 978-1-4832-2946-1.
20. Harlow, E.; Lane, D. P. *Antibodies: A Laboratory Manual*; 1 edition.; Cold Spring Harbor Laboratory Press, 1988; ISBN 978-0-87969-314-5.
21. Stafford, W. F.; Braswell, E. H. Sedimentation velocity, multi-speed method for analyzing polydisperse solutions. *Biophys. Chem.* **2004**, *108*, 273–279, doi:10.1016/j.bpc.2003.10.027.
22. Bjellqvist, B.; Ek, K.; Giorgio Righetti, P.; Gianazza, E.; Görg, A.; Westermeier, R.; Postel, W. Isoelectric focusing in immobilized pH gradients: Principle, methodology and some applications. *J. Biochem. Biophys. Methods* **1982**, *6*, 317–339, doi:10.1016/0165-022X(82)90013-6.
23. Mao, Q.; Pawliszyn, J. Capillary isoelectric focusing with whole column imaging detection for analysis of proteins and peptides. *J. Biochem. Biophys. Methods* **1999**, *39*, 93–110, doi:10.1016/S0165-022X(99)00006-8.
24. Hayes, D.; Laue, T.; Philo, J. *Program Sednterp: Sedimentation Interpretation Program version 1.09.*; Alliance Protein Laboratories: Thousand Oaks, CA, USA, 1995;
25. Edsall, J. T.; Wyman, J. *Biophysical chemistry*; Academic Press: New York, 1958; ISBN 978-0-12-232201-3.
26. Laue, T. Charge matters. *Biophys. Rev.* **2016**, *8*, 287–289, doi:10.1007/s12551-016-0229-3.
27. Tomar, D. S.; Kumar, S.; Singh, S. K.; Goswami, S.; Li, L. Molecular basis of high viscosity in concentrated antibody solutions: Strategies for high concentration drug product development. *mAbs* **2016**, *8*, 216–228, doi:10.1080/19420862.2015.1128606.
28. Saluja, A.; Fesinmeyer, R. M.; Hogan, S.; Brems, D. N.; Gokarn, Y. R. Diffusion and sedimentation interaction parameters for measuring the second virial coefficient and their utility as predictors of protein aggregation. *Biophys. J.* **2010**, *99*, 2657–2665, doi:10.1016/j.bpj.2010.08.020.
29. Laue, T. Proximity energies: a framework for understanding concentrated solutions. *J. Mol. Recognit. JMR* **2012**, *25*, 165–173, doi:10.1002/jmr.2179.